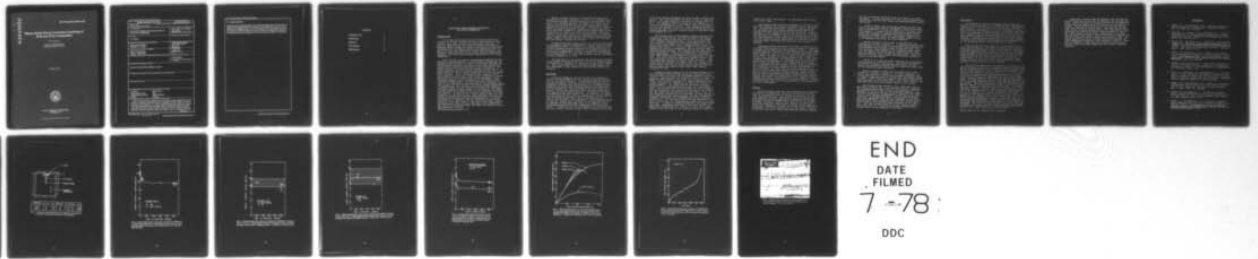


AD-A049 058 NAVAL RESEARCH LAB WASHINGTON D C F/G 11/6
SHARP NOTCH STRESS CORROSION CRACKING OF B/AL AND G/AL COMPOSIT, ETC (U)
OCT 77 W L PHILLIPS
UNCLASSIFIED NRL-MR-3616 N/L

1 of 1
AD
A049 058



END
DATE
FILMED
7-78
DDC

AD A049058

NRL Memorandum Report 3616

Sharp Notch Stress Corrosion Cracking of B/Al and G/Al Composites

W. L. PHILLIPS

*Composite Materials Branch
Engineering Materials Division*

October 1977



NAVAL RESEARCH LABORATORY
Washington, D.C.

Approved for public release: distribution unlimited.

20. Abstract (Continued)

for salt water and air exposures, analyses of the crack-opening-displacement versus time data, and appearances of the fracture surfaces, it is concluded that the delayed time failures in B/Al were caused by room temperature creep. For the G/Al composite, load carrying capacity was reduced about 25% due to 1000 hour immersion in salt water. Delayed time failures were attributed to the combined effects of room temperature creep and pitting corrosion adjacent to the crack tip.

CONTENTS

INTRODUCTION	1
PROCEDURE	2
RESULTS	4
DISCUSSION	6
REFERENCES	8

SHARP NOTCH STRESS CORROSION CRACKING OF B/Al AND G/Al COMPOSITES

INTRODUCTION

It is well established that the stress corrosion resistance of wrought aluminum alloys is determined by alloy content, heat treat history and load/crack direction. It would be expected that the stress corrosion resistance of aluminum matrix composites would be influenced by these same variables plus the added complications associated with the quality of the bond between the fibers and the matrix, the diffusion reactions which occur during elevated temperature exposure, and the stress corrosion resistance of the fibers themselves.

Over the past ten years, considerable research has been devoted to the development of boron/aluminum composites for aerospace applications, but most of this effort has been directed toward increasing the specific strength and specific modulus while retaining acceptable impact resistance. The effort devoted to evaluating the corrosion properties of these materials has been minimal considering that one of the major potential uses of these composites is on carrier based naval aircraft. Prior to beginning this research, there were reasons to think that, under certain conditions, stress corrosion could be a problem with these materials. First, corrosion studies of B/Al composites in unstressed conditions have shown severe, but very localized, corrosive attack at the fiber/matrix interface and at the diffusion bond line between the foil layers in diffusion bonded composites.^{1,2} In another paper, little interface corrosion was reported.³ Interface corrosion would reduce the strength of the composite when tensile stresses normal to the corroding interface were present. By definition, fracture would occur by stress corrosion if the material had a lower strength when the corrodent and stress were applied simultaneously than when the corrodent and stress were applied sequentially. It should be pointed out, however, that the localized corrosion was reported in the early 1970's, and, since that time, progress has been made in the diffusion bonding of B/Al composites. The better the diffusion bond, the lower the chance of interface corrosion failures.

Note: Manuscript submitted September 16, 1977

Second, stress corrosion of uniaxially aligned B/Al composites have been evaluated in a salt spray chamber with the tensile stresses applied parallel to the specimen fiber axis.⁴ The residual strength of B/6061 Al in both the as fabricated and T6 conditions was unaffected by salt spray exposure for periods up to one month. B/2024-T6 Al showed a slight decrease in residual strength with increasing exposure time while B/2024-F Al experienced complete matrix disintegration in a period of less than one month. Care was taken to electrically isolate the aluminum matrix composite from the steel load fixture but condensation inside the salt spray chamber could have galvanically coupled the specimen and the fixture, causing the failure.

Graphite/aluminum composites are in a much earlier stage of development than B/Al composites. Concern over the electrochemical potential difference which exists between G and Al has stimulated several studies on the corrosion properties of G/Al composites^{1,4,5} and on the corrosion properties of wrought aluminum when attached to graphite fiber/polymer matrix composites.^{6,7,8} There was no known work on the stress corrosion properties of G/Al.

The objective of this research was to evaluate the sharp notch stress corrosion properties of diffusion bonded plates of B/6061-T6 Al, B/6061-F Al, B/2024-F Al and G/201 Al/2024-F Al. Tests were conducted on transverse loaded compact tension specimens in both laboratory air and salt water environments.

PROCEDURE

Diffusion bonded 6.4 mm (0.25 inch) thick plates of B/6061-F Al and B/2024-F Al were fabricated using aluminum foil as the matrix material. The reinforcement was 50 vol %, uniaxially aligned, 0.142 mm (0.0056 inch) diameter boron filaments which had been manufactured by the chemical vapor deposition of boron onto a heated tungsten wire substrate. Both the B/6061-F Al and the B/2024-F Al were tested as received, with no heat treatment other than that associated with the diffusion bonding process. In addition, one plate of B/6061-F Al was heat treated to a T6 condition by subjecting the material to a solution temperature of 504 C (940 F) for 15 minutes, quenching in water, and aging at 160 C (320 F) for 18 hours. This procedure, which deviates slightly from the typical heat treatment for wrought 6061-T6 Al,⁹ is designed to give T6 properties to the composite while minimizing objectionable high temperature diffusion reactions.¹⁰ Suitability of the non-standard heat treatment was verified by heat treating wrought 6061 Al coupons and by four

point bend testing specimens cut from the heat treated composite. The coupon hardness was R_B 55, which is within the R_B 47 to 72 range reported as typical for wrought 6061-T6 Al.¹¹ The measured fracture stress for the composite in a direction perpendicular to the fibers, which is the weak direction, was 450 MPa (65.2 ksi). This compares favorably with values reported in the literature for B/6061-T6 Al and greatly exceeds a typical fracture stress of 120 MPa (17 ksi) for B/6061-F Al.^{12,13}

The graphite/201 aluminum/2024 aluminum composite was prepared by liquid metal infiltrating Thornel 50 graphite fibers with a 201 Al casting alloy to form 1.6 mm (0.063 inch) diameter impregnated tows. These impregnated tows were uniaxially aligned and diffusion bonded into 6.4 mm (0.25 inch) thick plates with a graphite fiber content of approximately 28 vol %. Layers of 2024 Al foil were placed between the layers of impregnated tows to minimize fiber breakage during bonding. The material was not heat treated after fabrication. Since G/Al composites are undergoing rapid improvements in mechanical properties, unnotched 4-point bend strengths were measured to characterize the material. The axial fracture stress was 675 MPa (98 ksi) and the transverse fracture stress was 64 MPa (9.3 ksi). This transverse bend strength is higher than the typical transverse tensile strength of 35 MPa (5 ksi) but, because of a surface foil layer and the nonuniform stress distribution, bend strengths are almost always higher than tensile strengths in G/Al.

Stress corrosion properties of precracked compact tension specimens were evaluated using the dead weight load fixture shown in Figure 1 and the sample geometry shown in Figure 2. Because holes are difficult to drill in B/Al, the specimens were loaded at the crack line using two steel links. One link was attached to a take-up mechanism which could be adjusted to compensate for small differences in sample geometry. The other link was attached, through a pivoted 10 to 1 load magnification arm, to a dead weight load. The figures show that the fibers were all aligned in the same direction, the cracks were parallel to the fibers, and the loads were perpendicular to the fibers. That is, the loads were applied in the transverse, or weak, direction. This orientation was chosen because, for most filamentary composite structures, the toughness and stress corrosion properties in the transverse direction were expected to be more critical than the corresponding properties in the axial direction. In order to conserve material, two sample sizes were used. Dimensions were chosen such that four of the smaller 35 mm by 33 mm (1.4 inch by 1.3 inch) test pieces could be cut from each of the fractured 74 mm by 70 mm (2.9

inch by 2.7 inch) test pieces. All specimens were 6.4 mm (0.25 inch) thick.

Dead weight load tests were conducted in 3½% salt water solution prepared from reagent grade NaCl and in laboratory air. For the salt water tests, galvanic coupling between the specimens and the loading fixtures was prevented by keeping the steel grips out of the salt solution. General corrosion of the immersed material was prevented by coating the specimens with Pyseal, which is a low melting point wax. The areas adjacent to the crack were left uncoated to simulate the conditions which would exist in a plated or coated structure where the protective layer had been chipped or damaged.

Overload fracture toughness tests were conducted on a universal testing machine in an air environment to establish a reference for evaluating time dependent effects. The same specimen geometry was used for the overload and delayed time tests except for a few of the early overload specimens, which had a spark cut crack tip with a radius of about 0.02 mm (0.001 inch) instead of a fatigue cracked tip. Unlike high strength wrought metals, the toughness of B/Al in the axial direction is independent of notch sharpness provided the notch radius is less than a few tenths of a mm.¹⁴ Comparison of the spark cut and fatigue cracked data indicates that the transverse fracture toughness is also independent of notch sharpness, at least over the range studied, and no distinction has been made between the overload data from the spark cut and the fatigue cracked samples. Spark cutting was not used on specimens subjected to dead weight loading because steel from the eroded razor blade electrode used to produce the crack tip was deposited on the sample and this contamination could influence the corrosion results. Fatigue precracking was done on an electrohydraulic testing machine in an air environment.

RESULTS

Stress intensity factors, as determined using equations published for homogeneous, isotropic materials^{15,16} versus time to fracture are given in Figures 3 through 6 for the four materials studied. The "zero" time to fracture data were computed using the maximum loads measured during the overload fracture toughness tests, instead of the customary 5% offset criterion. Data to the right of the zero time axis were obtained by dead weight loading the specimens in either air, denoted by circles, or in salt water, denoted by rectangles. The solid symbols are for the larger 74 mm by 70 mm (2.9 inch by 2.7 inch) specimens and the open symbols

are for the smaller 35 mm by 33 mm (1.4 inch by 1.3 inch) specimens. An arrow attached to a data point indicates that the material did not fail within the time specified, usually 1000 hours.

Figure 3 shows that, at stress intensities less than 80% of the overload fracture toughness, there were no failures in B/6061-T6 Al within the 1000 hour time limit which was imposed. At higher stress intensities, there were delayed time failures in samples which were tested in salt water and in samples which were dead weight loaded in air. A comparison of the solid and open symbols reveals little or no specimen size effect for this composite.

Stress intensity versus time to fracture data for B/2024-F Al is given in Figure 4. A horizontal scatter band corresponding to the range in values which were measured in the overload tests has been drawn through the data. For this material, there appears to be a specimen size effect, with the larger test pieces having slightly greater load carrying capacity than the smaller test pieces. Toughness does not decrease significantly with sustained loading in either air or salt water.

Figure 5 is a plot of stress intensity as a function of time to fracture for B/6061-F Al. The results are similar to B/2024-F Al except the specimen size effect is much larger and separate horizontal scatter bands have been drawn for the large and small specimens.

Stress intensity versus time to fracture for G/201 Al/2024 Al is shown in Figure 6. For this composite, the larger specimens have significantly greater toughness than the smaller specimens and two curves have been drawn through the data. These curves are based on salt water exposure results because, for the loads used in this study, none of the specimens which were dead weight loaded in air failed.

The maximum stress intensity for a 1000 hour life in salt water is about 75% of the overload fracture toughness. The corresponding stress intensity for exposure in air is estimated to be 80 to 85% of the overload toughness. This estimate is based on the data shown in Figure 6, interpretation of crack-opening-displacement versus time plots, and inspection of exposed specimens. This inspection showed that G/Al composites which had been immersed in salt water had developed large corrosion pits that were several millimeters deep in the uncoated region adjacent to the crack tip. The load carrying capacity of G/Al would be lower in salt water than in air due to the stress redistribution brought about by the presence of the pits.

DISCUSSION

Development of fracture toughness test methods and specimen size requirements for nonhomogeneous, nonisotropic composites is an active research area and many problems remain unsolved. Fortunately, it is not necessary to delay sharp notch stress corrosion research on composite materials until the problems in conducting and interpreting the fracture toughness tests have been worked out. By using the same specimen geometry for overload and dead weight tests, changes in load carrying capacity due to sustained loading in various environments can be measured and understood even if the toughness values are specimen size dependent.

Some insight into the nature of the specimen size effects can be obtained from stress intensity factor versus crack-opening-displacement (COD) curves measured during the overload toughness tests, as shown in Figure 7. Note that those specimens which had large nonlinear regions in their stress intensity/COD curves, in this case B/6061-F Al and G/201 Al/2024 Al, also had a significant size effect. B/6061-T6 Al, on the other hand, had a reasonably linear stress intensity/COD curve and no detectable size effect. B/2024-F Al fell between the two extremes.

For the B/Al composites, the similarity between the delayed time failure data for the samples tested in salt water and for samples tested in air suggests that the failures are due to room temperature creep. For the G/Al composite, the failures are probably also creep related but, in this case, there is the added complication associated with the deep corrosion pits which were observed after salt water immersion. Creep of composite materials has been studied by a number of researchers but most of this work has been carried out at elevated temperatures with loads applied parallel to the fibers. The room temperature creep of transverse loaded BORSIC*/1100 Al has been studied by Ericksen,¹⁷ who showed that the composite undergoes logarithmic creep, i.e. strain increases linearly with log time, at stresses greater than 55% of the fracture value. The logarithmic relationship is not valid, however, for strains approaching the tensile strength of the material and, at a given stress level, the BORSIC/1100 Al composite had a lower creep rate than the unreinforced matrix material. Figure 8 shows the plot of crack-opening-displacement versus time for the B/6061-T6 Al specimens that fractured after 60 hours in a salt water environment. The curve, which was obtained from a clip gage outputted to a digital printer, has the shape generally associated with high temperature creep failures.

*Trade name for SiC coated boron filaments.

Additional evidence that the delayed time failures are creep related may be obtained by examining the fracture surfaces. Figure 9 shows the fracture surface of the B/6061-T6 Al specimen that failed after 42 hours in a salt water environment. The fatigue precrack is on the left and the delayed time failure is on the right. Note that the delayed time failure involved separations at the fiber/matrix interfaces and the creation of deep troughs adjacent to each fiber, which appear as dark lines. According to the creep failure model, this lateral contraction would be required to maintain a constant matrix volume during plastic flow. Similarly appearing fracture surfaces have been reported for high temperature transverse creep failures of B/Al.¹⁸ There was no evidence of "mud cracked" patterns on the fracture surface, which are often associated with stress corrosion cracking.

REFERENCES

1. Evans, J.M., and Braddick, D.M., "Corrosion Behavior of Fibre-Reinforced Al Composites", Corrosion Science, Vol. 11, 1971, pp. 611-614.
2. Sedriks, A.J., Green, J.A.S. and Novak, D.L., "Corrosion Behavior of Aluminum-Boron Composites in Aqueous Chloride Solutions", Metallurgical Transactions, Vol. 2, March 1971, pp. 871-875.
3. Porter, M.C. and Wolff, E.G., "Corrosion of Boron-Metal Composites", Advances in Structural Composites, Vol. 12 (SAMPE), Society of Aerospace Materials and Process Engineers, 12th National Symposium and Exhibit, Anaheim, Calif., 1967, Paper AC-14.
4. Dardi, L.E. and Kreider, K.G., "Effect of Salt Water and High-Temperature Exposure on Boron-Aluminum Composites", Composite Materials: Testing and Design (Third Conference), ASTM STP 546, American Society for Testing Materials, 1974, pp. 269-283.
5. Kendall, E.G. and Dull, D.L., "Salt Water Corrosion Behavior of Aluminum-Graphite Composite", The Aerospace Corporation, Report No. TR-0074(9250-03)-2, SAMOS-TR-74-67, AD 777160, March 1974.
6. Dull, D.L., Harrigan, W.C. and Amateau, M.F., "The Corrosion of 6061 Aluminum Alloy-Thornel 50 Graphite Composite in Distilled Water and NaCl Solution", The Aerospace Corporation, Report No. TR-0075(5621)-2, SAMSO-TR-75-130, Contract F04701-74-C-0075, May 1975.
7. Brown, A.R.G. and Coomber, D.E., "Behavior of Couples of Aluminum and Plastics Reinforced with Carbon Fibre in Aqueous Salt Solutions", British Corrosion Journal, Vol. 7, Sept. 1972, pp. 232-235.
8. Fischer, P. and DeLuccia, J., "Effects of Graphite-Epoxy Composite Materials on the Corrosion Behavior of Aircraft Alloys", Naval Air Development Center Report No. NADC-75031-30, April 1975.
9. Fisher, P., and DeLuccia, J.J., "Effects of Graphite/Epoxy Composite Materials on the Corrosion Behavior of Aircraft Alloys", Environmental Effects on Advanced Composite Materials, ASTM STP 602, American Society for Testing and Materials, 1976.

10. The Aluminum Association, Aluminum Standards and Data, Third Edition, The Aluminum Association, New York, January 1972.
11. J. Dolowy, private communications.
12. ASM Handbook Committee, ASM Metals Handbook, Vol. 2, 8th Edition, American Society for Metals, 1964, p. 283.
13. Lynch, C.T. and Kershaw, J.P., Metal Matrix Composites, CRC Press, Cleveland, Ohio, 1972, p. 151.
14. Toth, I.J., "Comparison of the Mechanical Behavior of Filamentary Reinforced Aluminum and Titanium Alloys", Composite Materials: Testing and Design (Third Conference), ASTM STP 546, American Society for Testing and Materials, 1974, pp. 542-560.
15. Hoover, W.R. and Allred, R.E., "The Toughness of Borsic/Al Composites with Weak Fiber-Matrix Bonds", Failure Modes in Composites, AIME, 1973, pp. 311-326.
16. Brown, B.F., Stress Corrosion Cracking in High Strength Steels and in Titanium and Aluminum Alloys, U.S. Government Printing Office, 1972, pp. 32-34.
17. Brown, W.F. and Srawley, J.E., Plane Strain Crack Toughness Testing of High Strength Metallic Materials, ASTM STP 410, American Society for Testing and Materials, 1966, p. 14.
18. Ericksen, R.H., "Room Temperature Creep of Borsic-Aluminum Composites", Metallurgical Transactions, Vol. 4, July 1973, pp. 1687-1693.
19. Lucas, G.F. and McNelley, T.R., "A Comparison Between Creep of Laminated Aluminum and the Transverse Creep Behavior of a Unidirectional Boron-Aluminum Composite", Metallurgical Transactions, Vol. 7A, pp. 1317-1324.

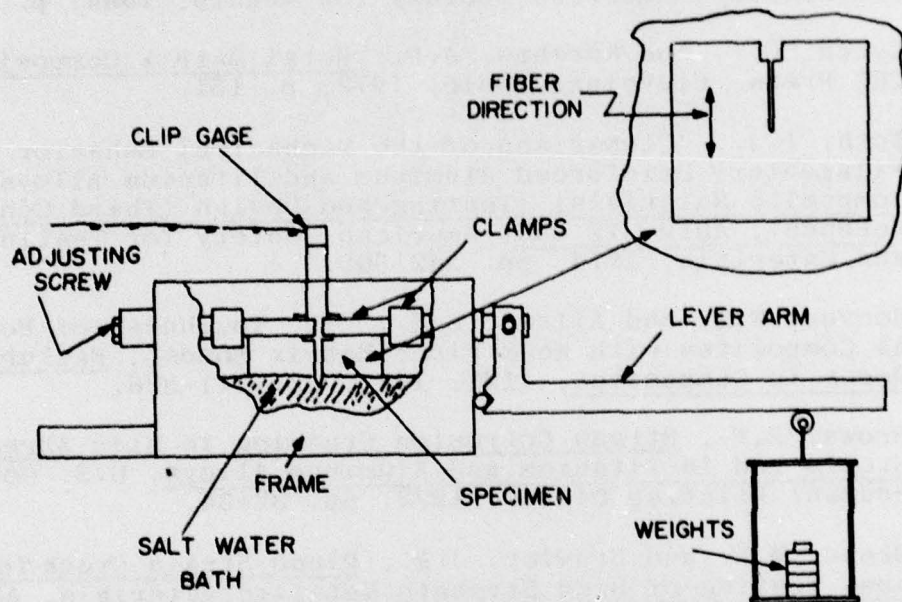
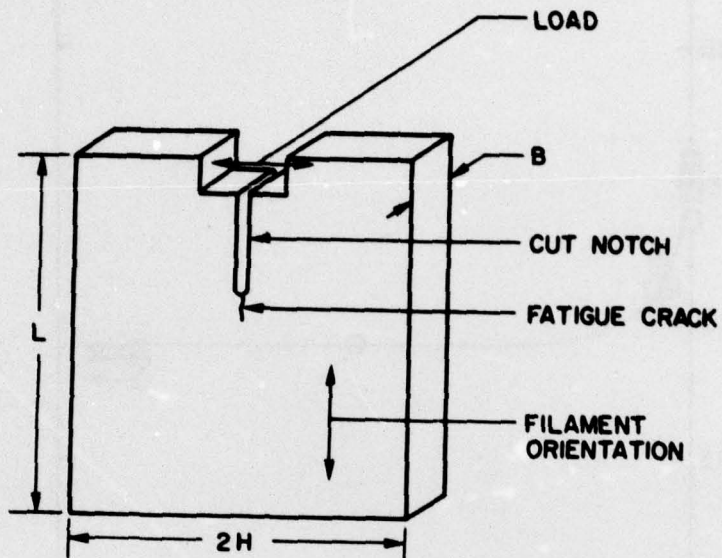


Fig. 1 — Fixture used to dead weight load uniaxially aligned B/Al and G/Al composites in salt water. For tests conducted in an air environment, the salt water was omitted.



SPECIMEN	L-mm	(in.)	2H-mm	(in.)	B-mm	(in.)
LARGE	74	(2.9)	70	(2.7)	6.3	(0.25)
SMALL	35	(1.4)	33	(1.3)	6.3	(0.25)

Fig. 2 — Compact tension specimens used to evaluate the overload and delayed time toughness of B/Al and G/Al composites

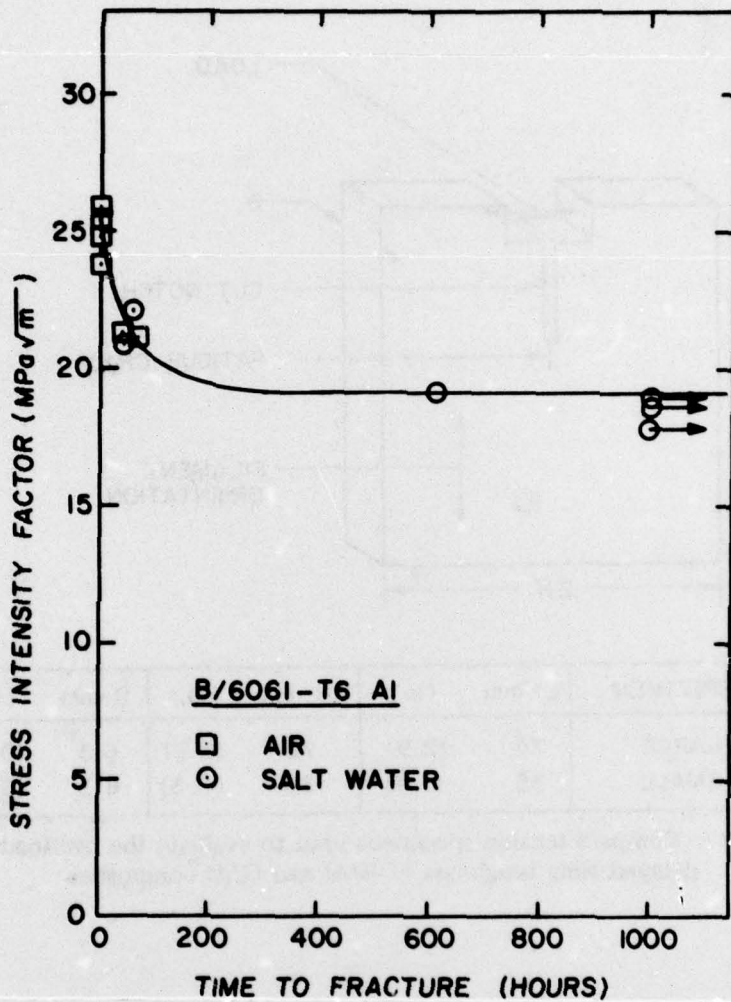


Fig. 3 - Stress intensity factor versus time to fracture for B/6061-T6 Al loaded in salt water and air. Large specimens are denoted by shaded and small specimens are denoted by unshaded symbols. (1 MPa \sqrt{m} = 0.910 ksi $\sqrt{in.}$).

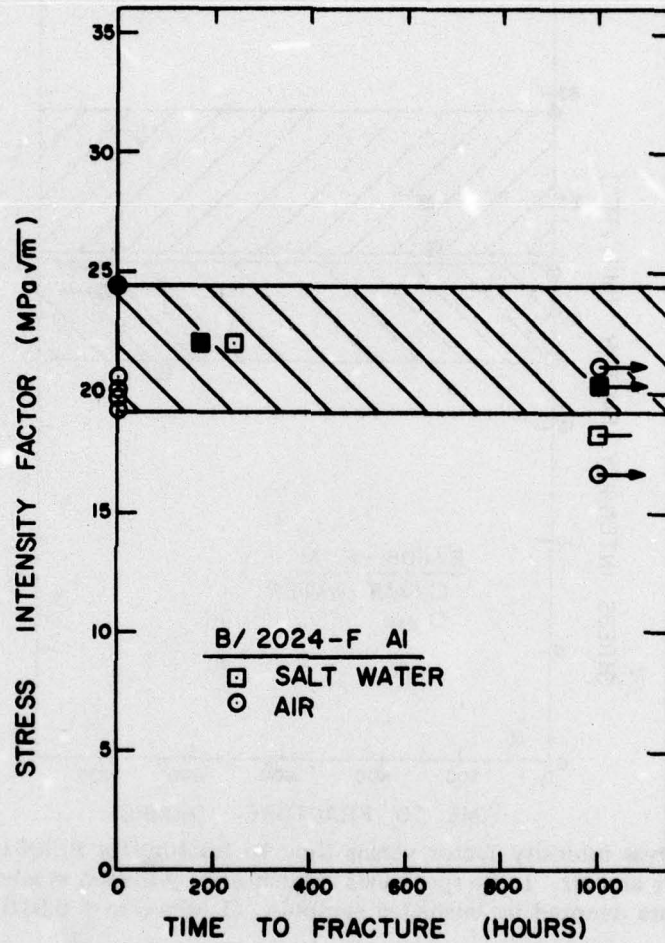


Fig. 4 - Stress intensity factor versus time to fracture for B/2024-F Al loaded in salt water and air. Large specimens are denoted by shaded symbols and small specimens are denoted by unshaded symbols. (1 MPa√m = 0.910 ksi√in.).

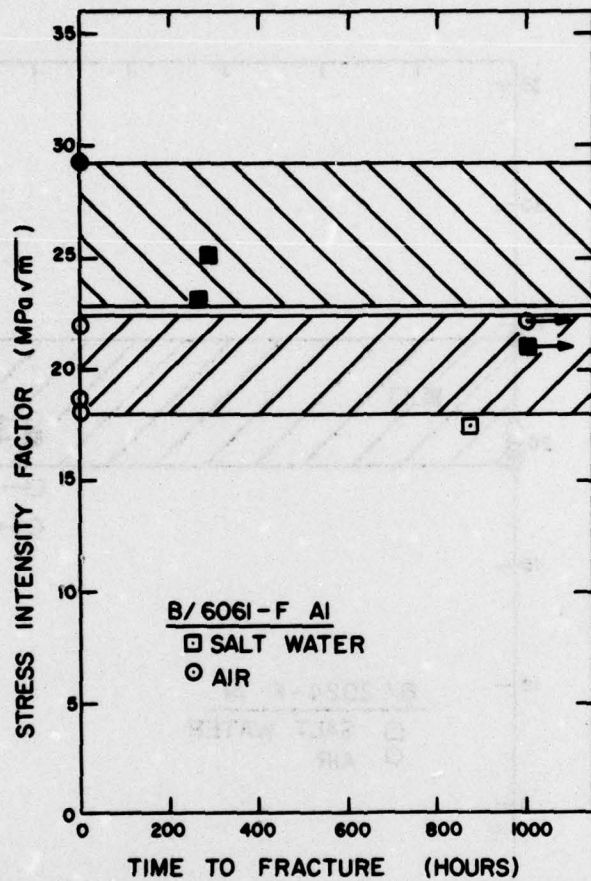


Fig. 5 — Stress intensity factor versus time to fracture for B/6061-F Al loaded in salt water and air. Large specimens are denoted by shaded symbols and small specimens are denoted by unshaded symbols. (1 MPa \sqrt{m} = 0.910 ksi $\sqrt{in.}$).

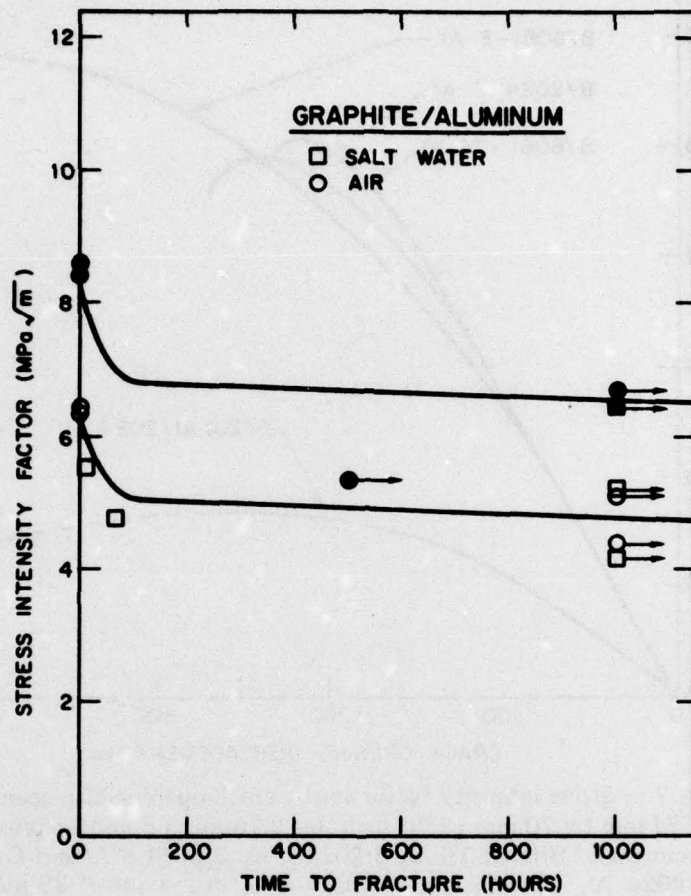


Fig. 6 — Stress intensity factor versus time to fracture for G/201 Al/2024 Al loaded in salt water and air. Large specimens are denoted by shaded symbols and small specimens are denoted by unshaded symbols. (1 MPa \sqrt{m} = 0.910 ksi $\sqrt{in.}$).

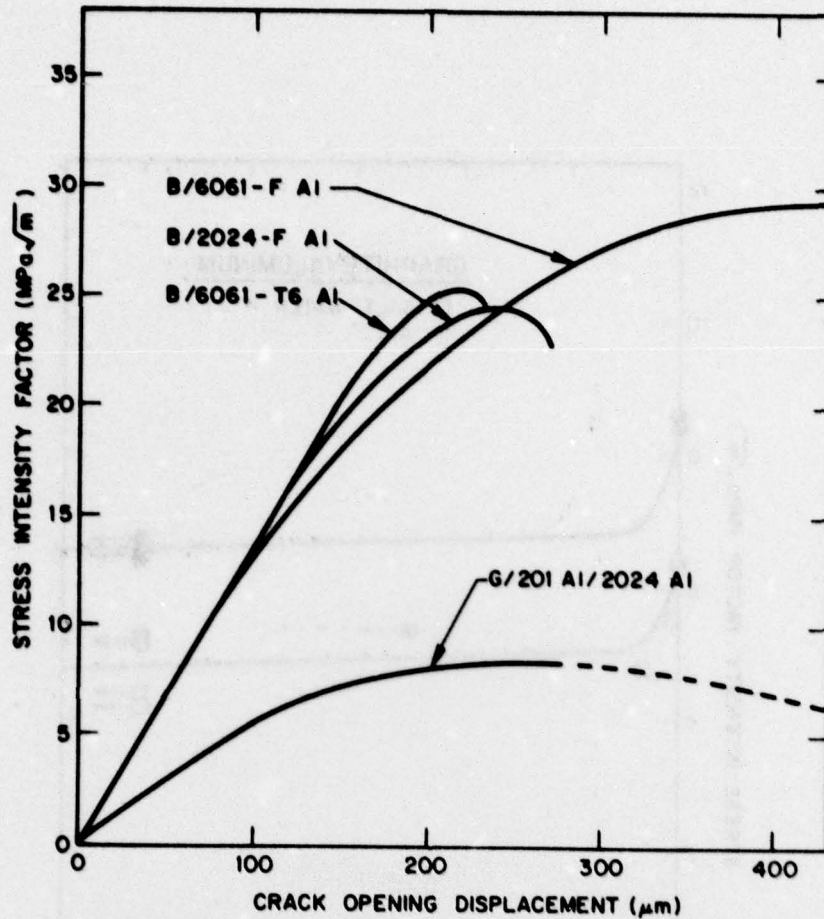


Fig. 7 - Stress intensity factor versus crack-opening-displacement for 74 mm by 70 mm (2.90 inch by 2.75 inch) compact tension specimens of B/6061-T6 Al, B/2024-F Al, B/6061-F Al and G/201 Al/2024 Al. (1 MPa \sqrt{m} = 0.910 ksi $\sqrt{in.}$, 1 μm = 39 μ inches).

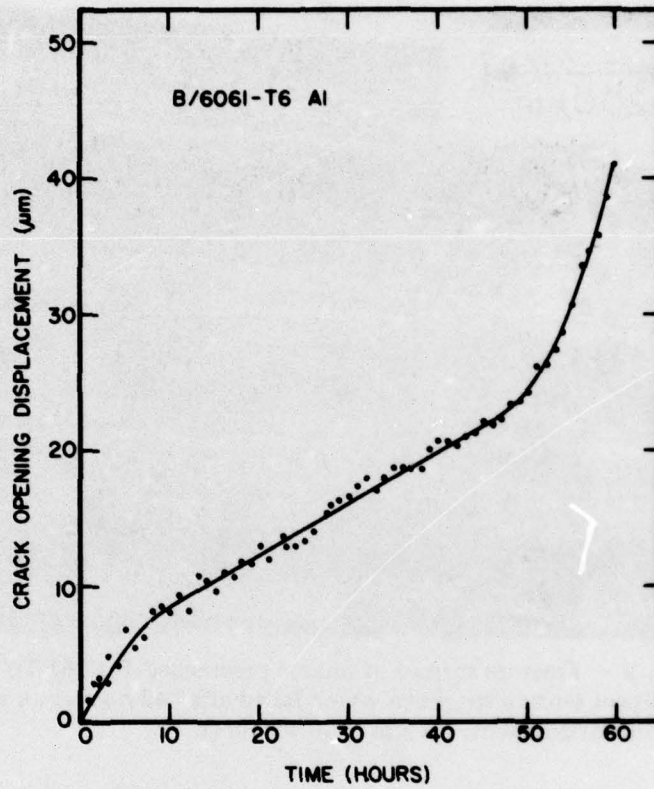


Fig. 8 — Crack-opening-displacement versus time for B/6061-T6 Al compact tension specimen dead weight loaded to a stress intensity factor of $22.1 \text{ MPa}\sqrt{\text{m}}$ ($20.1 \text{ ksi}\sqrt{\text{in.}}$) in a salt water environment. ($1 \mu\text{m} = 39 \mu\text{inches}$).

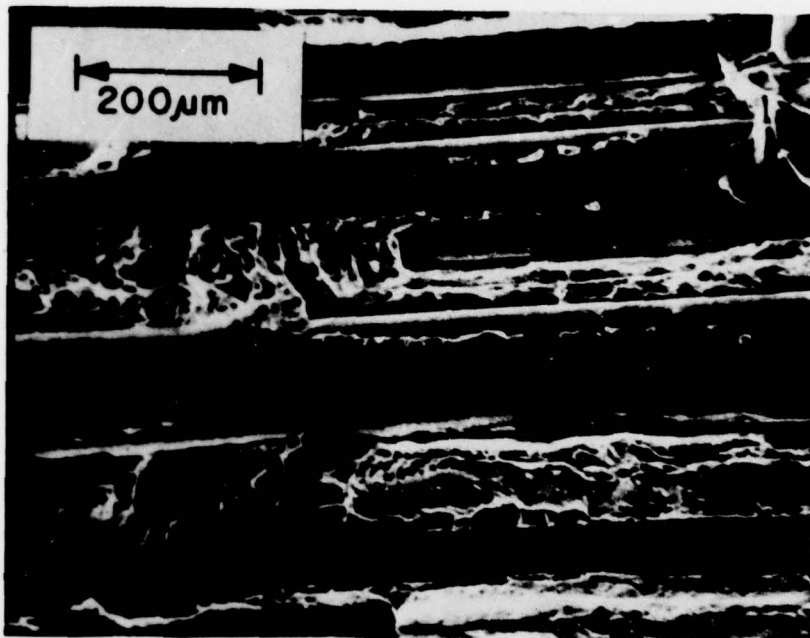


Fig. 9 — Fracture surface of fatigue precracked B/6061-T6 Al compact tension specimen which failed after 42 hours in a salt water environment. ($1 \mu\text{m} = 39 \mu\text{inches}$).